ACS APPLIED MATERIALS & INTERFACES

Letter

www.acsami.org

# Fabrication of Novel Transparent Touch Sensing Device via Drop-on-Demand Inkjet Printing Technique

Siyuan Ma,[†] Flavio Ribeiro,[†] Karlton Powell,[†] John Lutian,[†] Christian Møller,[†] Timothy Large,[†] and James Holbery*[,†]

[†]Applied Sciences Group, Microsoft Corporation, Redmond, Washington 98052, United States

Supporting Information

**ABSTRACT:** A novel transparent touch sensor was fabricated with a drop-on-demand inkjet printing technique on borosilicate glass and flexible polyethylene terephthalate (PET) substrates. Conductive poly(3,4-ethylenedioxythiophene):poly(styrenesulfonate) (PEDOT:PSS) and dielectric poly(methylsiloxane) were deposited on a desired area to form a capacitive touch sensor structure. The properties of the printed sensors (optical transparency, electrical resistance and touch sensing performance) were investigated with varying PEDOT: PSS printing passes. A novel transparent touch sensor fabricated with an all-inkjet-printing method is demonstrated for the first time. This process holds industrially viable potential to fabricate transparent touch sensors with an inkjet printing technique on both rigid and flexible substrates for a wide range of applications.

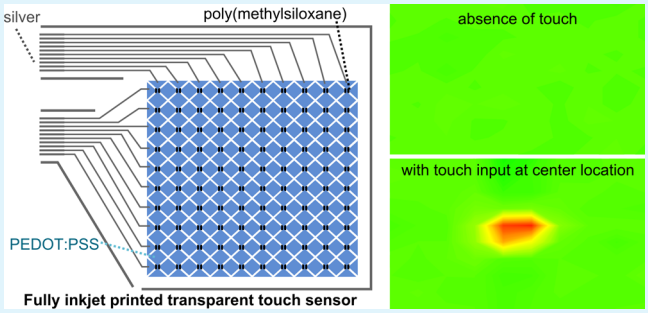


**KEYWORDS:** *inkjet printing, touch sensor, PEDOT:PSS, printed electronics, organic electronics, additive manufacturing*

Touch sensors have been widely investigated and employed in user interfaces of mobile displays. Techniques based on different mechanisms such as resistive,[1] surface acoustic wave,[2] infrared ray,[3] and capacitive[4,5] have been developed to sense touch inputs. Typical resistive touch sensors consist of two parallel layers of conductive material (electrodes), which are separated by a structured dielectric interlayer.[1] Resulting from a touch event, the two electrodes contact at a local point, resulting in a change of resistance that indicates the location of the touch. Resistive touch sensing mechanisms have been used on many commercial mobile touchscreens. However, its disadvantages include large activation force, mechanical aging due to cyclic structural deformation, and inherent optical artifacts because of light reflecting between electrode layers, restricting applications. Drawbacks of sensors based on surface acoustic wave and infrared ray techniques are attributed to their high cost, structural complexity, and false responses due to contaminants or light.[6] The rapid growth of capacitive touch sensors in commercial products is mainly attributed to their unlimited multitouch functionality, good mechanical robustness and relatively structural simplicity.[5,6] A general capacitive touch sensor consists of individual patterns of conductive electrodes intersected in perpendicular directions (along horizontal ($x$) and vertical ($y$) axis, respectively). The electrodes along x and $y$-axis are distributed on either a same substrate with dielectric separator at the local intersection, or on two individual parallel substrates which are separated by a continuous dielectric layer.[5] Capacitors are formed by the intersected electrodes ($x$–$y$ electrodes). If a conductive and capacitively grounded object (e.g., a human finger) is placed near an intersection of x-y electrodes, the capacitance value changes due to the disturbance of the fringing electric field in the neighborhood of the intersection. Indeed, electric field lines which would exist between the $x$ and $y$ electrodes are diverted to the finger, decreasing the capacitance between the electrodes.[7] The capacitance values at all $x$–$y$ electrode intersections are constantly measured by an electrical sensing circuit. Location of touch inputs are estimated based on measured capacitance decrease at specific positions.[5,7]

Low electrical resistance of electrodes is desirable to enable fast circuit measuring time and high signal-to-noise ratio.[7] Optical transparency is also an important property when the touch sensor is over a display. Indium tin oxide (ITO), a transparent conductive material, has been the industrial standard employed in large-scale manufacturing for many optoelectronic applications including touch screens.[8] ITO electrodes for a capacitive touch sensor are generally realized via a lithography-based subtractive patterning process which has inherent drawbacks such as high cost, large amount of waste, mask requirement, and slow and complex manufacturing process.[9,10] The apparent disadvantages of ITO have also been well recognized- the issues of indium scarcity, high cost and its inherent mechanical brittleness.[11] Poly(3,4-ethylenedioxythiophene):poly(styrenesulfonate) (PE-

**Received:** May 29, 2015
**Accepted:** September 21, 2015
**Published:** September 21, 2015





DOI: 10.1021/acsami.5b04717
*ACS Appl. Mater. Interfaces* 2015, 7, 21628–21633

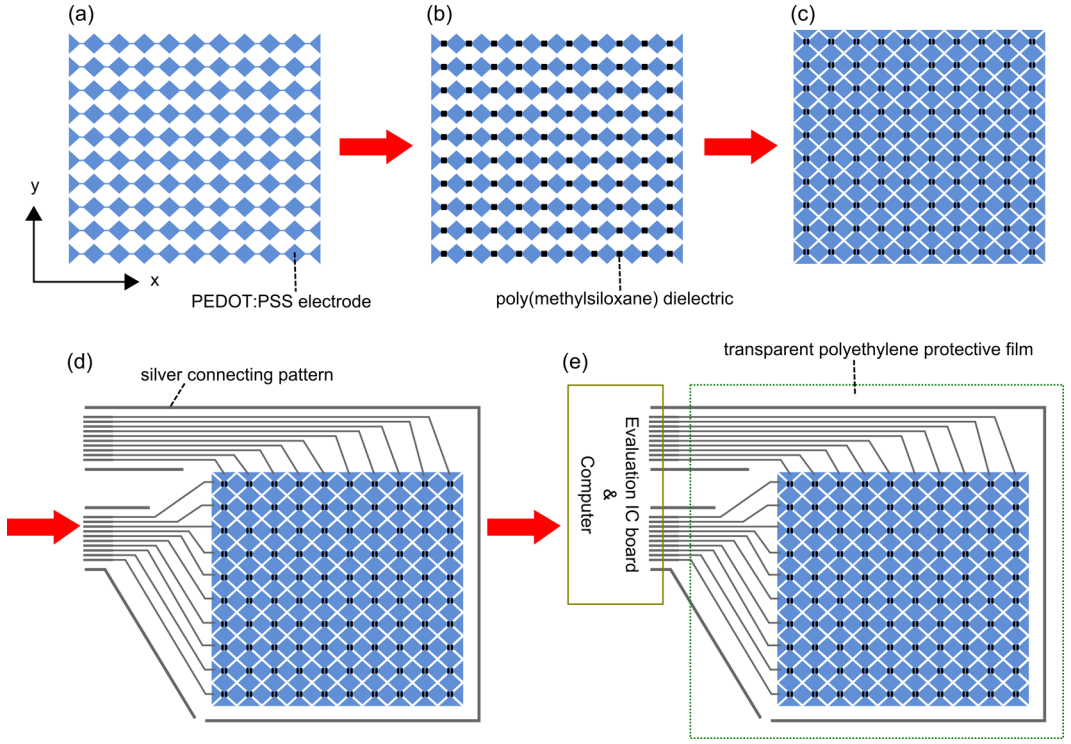


**Figure 1.** Schematic of transparent touch sensor inkjet fabrication process: (a) inkjet print poly(3,4-ethylenedioxythiophene):poly(styrenesulfonate) (PEDOT:PSS) electrode patterns along horizontal direction (*x*- axis); (b) poly(methylsiloxane) dielectric separator fabrication by inkjet printing methylsiloxane suspension and subsequent thermal curing; (c) inkjet print PEDOT:PSS electrode patterns along vertical direction (*y*- axis); (d) inkjet print conductive silver pattern for connection; (e) laminate a transparent polyethylene film and connect the sensor to a IC board for sensing performance evaluation.

DOT:PSS) is believed to be a possible material candidate for ITO replacement for a variety of its merits.[12] Its highly transparence, conductivity and mechanical flexibility make it an ideal electrode material for ITO-free transparent touch sensor structures.[13]

Solution-based manufacturing techniques such as drop-on-demand (DOD) inkjet printing,[9] gravure printing,[14] slot die coating[15] and screen printing[16] have been widely employed to deposit electrically functional structures on both rigid and flexible substrates. Among them, DOD inkjet printing is an outstanding candidate because of its additive manufacturing attributes that include superior material utilization, low process temperature and a mask-independent process that can be easily incorporated into large-scale roll-to-roll (R2R) manufacturing infrastructures for flexible substrates.[17] The structures fabricated by the DOD inkjet printing technique have exhibited significant potential for a wide range of applications such as solar cells,[18,19] batteries,[20,21] antennas,[16,22] and thin film transistors.[23−25] Touch sensing buttons fabricated by inkjet printing have been reported based on depositing silver patterns on paper substrates.[26,27] However, there is no previous work in the public domain regarding transparent touch sensor fabrication employing the inkjet printing technique.

In this study, we report the first demonstration of drop-on-demand (DOD) inkjet printing as a viable method to fabricate transparent touch sensors. An aqueous dispersion of conductive polymer- poly(3,4-ethylenedioxythiophene):poly-(styrenesulfonate) (PEDOT:PSS) was printed to fabricate transparent electrode patterns as an alternative to indium tin oxide (ITO). A thermally curable methylsiloxane dispersion was printed to create transparent dielectric structures. The transparent touch sensors were fabricated on borosilicate glass and polyethylene terephthalate (PET) substrates with a maximum processing temperature of 140 °C. We investigated the effects of PEDOT:PSS printing passes on optical transparency, electrical resistance and sensing performance of the fabricated touch sensors.

The fabrication process starts with an inkjet printing of PEDOT: PSS aqueous dispersion (Clevios P Jet V2, Heraeus Holding GmbH, Hanau, Germany) to form individual electrodes along horizontal axis (*x*-axis) on a 100 mm × 100 mm substrate (either borosilicate glass or PET) (Figure 1(a)). Each electrode consists of connected diamond-shaped patterns with a 2.46 mm edge length. The entire length of each electrode is 40 mm. The dielectric ink- silica particles filled methylsiloxane dispersion, which is a mixed system containing a latent heat-cure catalyst (Perma 6000, CA Hardcoating, Chula Vista, CA, USA), is then printed to form square patterns (1.00 mm edge length) (Figure 1b). Thermal curing was applied to solidify the dielectric ink, resulting in insulating separators. Individual electrodes along substrate vertical direction (*y*-axis) are printed using the same PEDOT: PSS ink (Figure 1c). The insulating separators ensure no electrical connections at junctions of any intersected electrodes along *x* and *y* axes. This entire pattern is recognized as an "interlocking diamond" sensor structure, which has been widely used in many commercial applications.[28] Then silver nanoparticle suspension ink (DGP 40LT- 15C, ANP, Sejong, Korea) was printed and subsequently sintered to form the pattern for sensor connection (Figure 1d). After laminating a transparent polyethylene film (7524T11, McMaster, Elmhurst, IL, USA) for structure protection, a touch sensor evaluation IC board (mXT1664S,


DOI: 10.1021/acsami.5b04717
ACS Appl. Mater. Interfaces 2015, 7, 21628−21633

Atmel, San Jose, CA, USA) was connected to the silver pattern for sensor performance characterization (Figure, 1e). For details of substrate preparation, inkjet printing apparatus, printing process, and postprinting treatment, please see the Supporting Information.

Photos of typical touch sensor photos that were fabricated by printing various number of PEDOT:PSS printing passes are exhibited (Figure 2a). A sensor printed with a single pass of

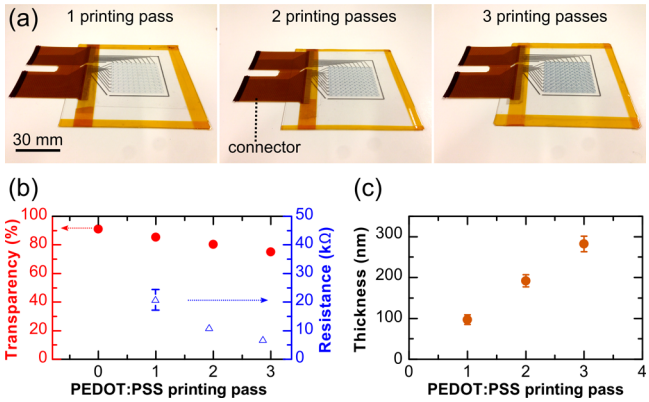


**Figure 2.** Structural, optical, and electrical characterization with various number of PEDOT:PSS printing passes: (a) camera photos of typical touch sensor structure; (b) optical transparency in sensing region and electrical resistance of each electrode; (c) PEDOT:PSS layer thickness.

PEDOT:PSS shows the least structural visibility in the sensing area. The structural apparentness enhances with increasing printing pass of the PEDOT:PSS pattern.

The influence of each PEDOT:PSS printing pass on device optical transparency was measured by a spectrophotometer at the sensing area (SP-200, Orb Optronix, Kirkland, USA) (Figure 2b). The substrate shows transparency of about 91% with absence of any deposited structures. For a touch sensor fabricated by printing a single pass of PEDOT:PSS, it maintains a transparency of about 85%. Transmittance decreases approximately 5% with each additional printing pass. Electrical resistance also decreases with increasing PEDOT:PSS printing pass (Figure 2b). For a single-pass-printed PEDOT:PSS electrode, the resistance between two ends of an electrode is about 20.8 kΩ. The minimal value achieved is 6.9 kΩ, which was measured for electrodes fabricated with 3 printing passes.

The thickness of the printed PEDOT:PSS electrodes was measured with a 3D laser scanning confocal microscope (VK-X200, Keyence, Itasca, USA) (Figure 2c). The thickness value increases linearly with increasing printing passes. An approximately 100 nm thick structure is added for each printing pass. The thickness increase explains the trends of resistance and transparency change as shown in Figure 2b. The thickness of the dielectric pattern was measured as 4720 ± 380 nm, a much greater value than the PEDOT:PSS electrode thickness.

The morphology of the printed structure was characterized by optical microscopy (Zeta-20, Zeta Instruments) and scanning electron microscopy (SEM) (JSM7400F, JEOL, Peabody, USA) (Figure 3). The optical microscope image shows an intersection of two PEDOT:PSS electrodes printed along horizontal and vertical directions, which are separated by a dielectric pattern (Figure 3a). It is observed that the PEDOT:PSS deposited on the dielectric surface is rough with a high degree of irregularity as compared to patterns deposited

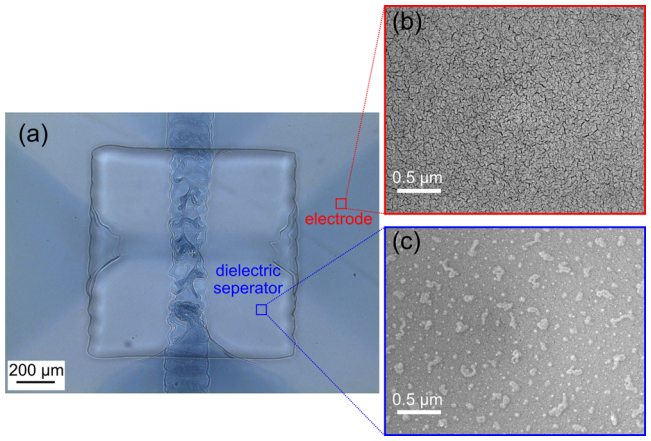


**Figure 3.** Typical microscope images of (a) optical microscope image of an intersection of two electrodes printed along horizontal and vertical directions, separated by a dielectric square pattern; (b, c) scanning electron microscope (SEM) images of printed electrode and dielectric regions, respectively. The lines with indicating squares show the approximate regions that are observed at higher magnification by SEM.

on substrate (Figure 3a). This can be explained by different surface energies and the resulting different ink wetting behaviors on the varied material surfaces (Supporting Information). Typical SEM image at the electrode region exhibits uniform and dense PEDOT:PSS structure. In contrast, SEM images at the dielectric separator area shows morphology of a fine background mixed with granular aggregates. It is likely that the continuous and granular phases are poly-(methylsiloxane) and silica particle aggregates, respectively, in accordance with the ink compositions.

Touch input on sensors was visualized by characterizing the printed structures via a sensor performance evaluation IC board with associated software (mXT1664S, Hawkeye Software, Atmel, San Jose, CA, USA). The capacitance values are measured and expressed in analog-digital converter (ADC) counts. The capacitance at each position of the intersected $x-y$ electrodes is measured first with the absence of touch input. The measured capacitance is defined as reference capacitance ($C_o$). When touch is applied, the capacitance at the local touched position is defined as $C_i$. The sensor performance evaluation IC circuitry with its associated software measures values of $C_o - C_i$ at each intersection constantly, and outputs the values in ADC counts. With absence of any touch input, $C_o - C_i$ is close to zero value as $C_o = C_i$. And at local touch applied positions, $C_o - C_i$ yields a positive count value as $C_i < C_o$.[5,6] As expected, values of $C_o - C_i$ are measured close to zero on the entire sensor surface with absence of touch input (Figure 4a). The printed sensor is capable of identifying touch events from single-position and multiposition touches at various locations (Figure 4a). For the multitouch input (Figure 4a), both positions on lower left and upper right of a representative sensor are touched simultaneously. The sensor detects the touch inputs accurately at the corresponding locations (Figure 4a). The corresponding negative values of $C_o - C_i$ are shown in the upper left and lower right regions of the sensing area. This is a well-known electrical artifact for capacitive multitouch sensors called signal retransmission. The origin of this artifact is due to the hand providing a parasitic impedance between the fingers, allowing an electrode $y_1$ under touch #1 to receive charge from an electrode $x_2$ under touch #2, even though $y_1$ is


DOI: 10.1021/acsami.5b04717
ACS Appl. Mater. Interfaces 2015, 7, 21628−21633

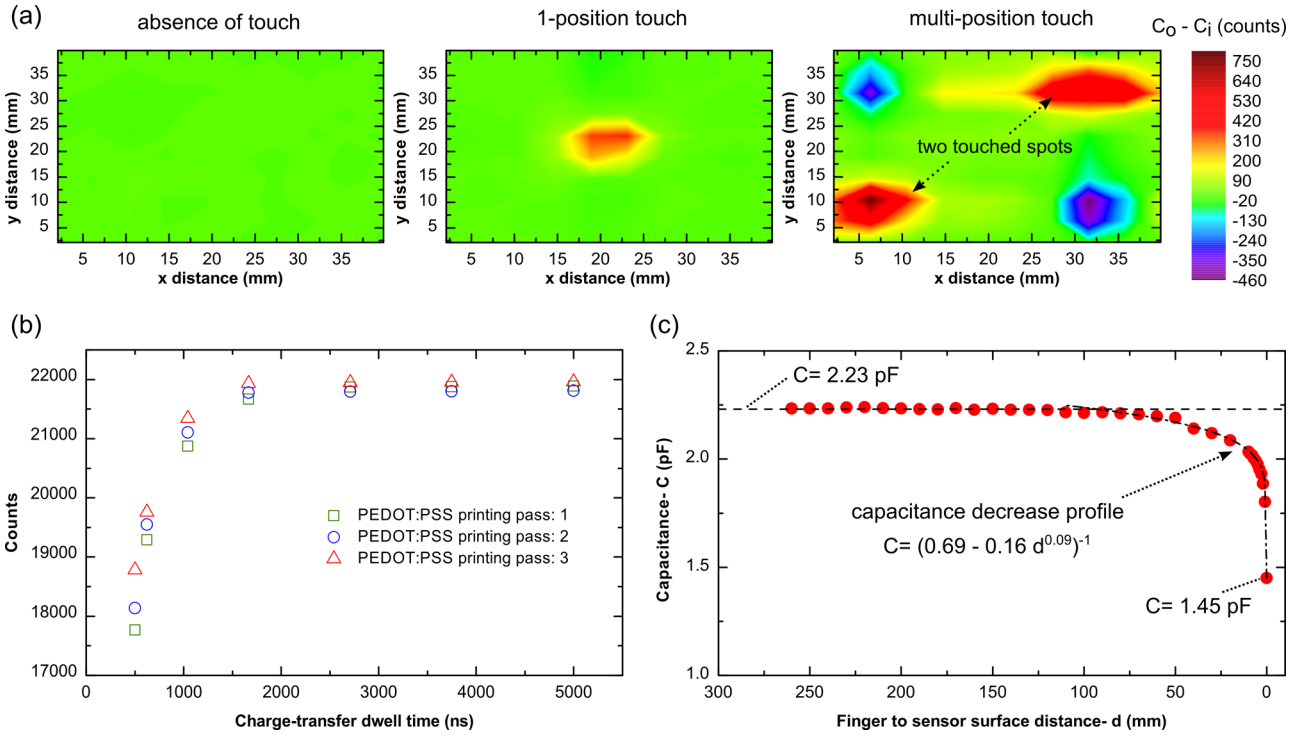


**Figure 4.** Device touch sensing characterization: (a) touch events visualization of a typical sensor fabricated by printing 1 pass of PEDOT:PSS ($C_o$ and $C_i$ are the capacitance in analog counts without and with touch input at the position of intersected PEDOT:PSS electrodes); (b) electrical signal acquisition of sensors with various PEDOT:PSS printing passes; (c) measured capacitance value ($C$) at an electrode intersection, as a function of distance between the sensor surface and a finger placed above in proximity.

not under touch #2. These additional charges cause the capacitance at $(x_2,y_1)$, an electrode intersection with no touches, to be overestimated. This artifact is not highly influential, because the algorithm of the sensing evaluation program can be set to ignore the artifact positions by only considering positive values of $C_o - C_i$ on the sensor area. A video of a representative sensor under evaluation is included in the Supporting Information.

The influence of the number of PEDOT:PSS printing passes on signal settling time was characterized by the same evaluation IC board technique. For each fabricated sensor, ADC counts representing the reference capacitance were recorded with varying charge-transfer dwell time, in the absence of touch input (Figure 4b). The charge-dwell time is the time the measurement circuit waits between driving an excitation and performing an ADC measurement representative of the capacitance between x-y electrodes. For a general touch sensor, too short a charge-transfer dwell time induces inadequate charge collection and therefore produces low signal counts. Indeed, the circuit under test is well characterized by an RC (resistor-capacitor) series model, with a step response given by $V_C(t) = V(1 - e^{-t/RC})$, where $V_C$ is the voltage across the capacitor, t the time, V the source voltage, $R$ the resistance and $C$ the capacitance. Thus, the charge-transfer dwell time should be sufficiently large with respect to the RC product. It is desirable to measure high ADC counts with short charge-dwell times, as it indicates a sensor with low resistance and thus short settling time. In Figure 4b, at charge-transfer dwell time shorter than 2000 ns; an increase in signal counts is observed for each sensor printed with the same pass of PEDOT:PSS pattern. At long charge-transfer dwell times (>2000 ns), maximum signal counts are obtained by each sensor, indicating effective charge transfer within the defined charge-transfer dwell times (Figure 4b). At the shortest charge-transfer dwell time (500 ns), a large difference between the collected signal counts is observed among the sensors printed with various passes of PEDOT:PSS. And the differences are minimized with increasing charge-transfer dwell time, resulting in very minor variance among sensors at dwell times longer than 2000 ns. Increased signal counts are generally obtained with increasing PEDOT:PSS printing passes at the same charge-transfer time (Figure 4b). This is explained by the decreased electrode resistance value with increasing PEDOT: PSS printing pass as shown in Figure 2b.

The capacitance value at an $x-y$ electrode intersection was characterized with an LCR meter (E4980A, Agilent Technologies, Santa Clara, CA). A capacitance value of 2.23 pF was recorded with the absence of object above the sensor. A grounded metal bar with 12.5 mm diameter was used to simulate a human finger, and was attached to a height-adjustable stage that ensures accurate control of the distance between the simulating finger and sensor surface (d). When the simulated finger is far above sensor surface ($d$ > 120 mm), the capacitance value maintains a constant value as 2.23 pF - equivalent to the value with absence of object above the sensor. Capacitance decreases when the simulated finger approaches the sensor surface from a distance less than 120 mm ($d$ < 120 mm). The capacitance ($C$) decreases following a fitting equation $C = (0.69-0.16d^{0.09})^{-1}$ to a value of 1.45 pF when the simulating finger touches sensor surface ($d$ = 0). Decrease in capacitance indicates charges transferring from sensor capacitor to a finger, which is consistent with the mutual capacitance sensing mechanism.[5,6]

Photos of the same touch sensing structures printed on flexible PET substrate are shown with the structure in the flat and bent conditions (Figure 5). No sensing performance


DOI: 10.1021/acsami.5b04717
ACS Appl. Mater. Interfaces 2015, 7, 21628−21633

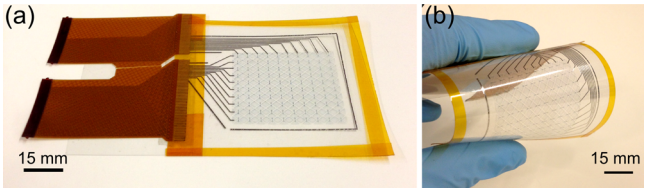


**Figure 5.** Images of a typical sensor inkjet fabricated on PET substrate with one printing pass of PEDOT:PSS electrodes under (a) unbent and (b) bent geometry.

degradation is observed of sensors on PET substrates subsequent to manually 100 cycles of bending test on a mandrel with 8 mm diameter. Comprehensive mechanical robustness characterization of sensors on PET substrates is under our current investigation.

In conclusion, novel transparent touch sensors were fabricated for the first time using an all-inkjet-print technique on glass and polyethylene terephthalate (PET) constructed of poly(3,4-ethylenedioxythiophene):poly(styrenesulfonate) (PEDOT:PSS) dispersions and thermally curable methylsiloxane. Increasing PEDOT: PSS printing passes from 1 to 3, sensor electrode resistance decreases from 20.8 to 6.9 kΩ; transparency decreases from 85 to 75%. Single-position and multitouch input visualization was realized using a sensor evaluation IC board technique with its embedded software. Signal settling time of sensors decreases with increasing PEDOT: PSS printing passes. The developed process demonstrates a simple, low temperature, and low-cost method of fabricating transparent touch sensing structures on both rigid and flexible substrates. Coupling with rapid development of solution-processed transparent conductive materials, this process potentially leads to a direction of fabricating transparent touch sensors with high sensing performance.

## ■ ASSOCIATED CONTENT

### Supporting Information

The Supporting Information is available free of charge on the ACS Publications website at DOI: 10.1021/acsami.5b04717.

Details of substrate preparation, inkjet apparatus, printing process, postprinting treatment (PDF)

Movie S1, touch input visualization (AVI)

## ■ AUTHOR INFORMATION

### Corresponding Author

*E-mail: jiholb@microsoft.com. Tel: +01 425-703-4482.

### Notes

The authors declare no competing financial interest.

## ■ ACKNOWLEDGMENTS

This research was supported by Microsoft Corporation. The authors thank Mr. Mike Sinclair at Hardware Lab of Microsoft Corporation for valuable discussion and technical support.

## ■ REFERENCES

(1) Eaton, W. P.; Smith, J. H. Micromachined Pressure Sensors: Review and Recent Developments. In *Smart Structures and Materials*; Varadan, V. K., McWhorter, P. J., Eds.; IOP Science: Philadelphia, PA, 1997; pp 30−41.

(2) Adler, R.; Desmares, P. J. An Economical Touch Panel Using SAW Absorption. *IEEE Trans. Ultrason., Ferroelect., Freq. Control* **1987**, *34*, 195−201.

(3) Han, S. Y.; Kim, D. C.; Cho, B.; Jeon, K. S.; Seo, S. M.; Seo, M. S.; Jung, S.-W.; Jeong, K.; Kim, W. K.; Yang, S.-H.; Kim, N.-H.; Song, J.; Kong, H.-S.; Kim, H. G. A Highly Sensitive and Low-Noise IR Photosensor Based on a-SiGe as a Sensing and Noise Filter: Toward Large-Sized Touch-Screen LCD Panels. *J. Soc. Inf. Disp.* **2011**, *19*, 855−860.

(4) Hotelling, S.; Strickon, J. A.; Huppi, B. Q. Multipoint Touchscreen. U.S. Patent 2006 7 663 607.

(5) Kim, S.; Choi, W.; Rim, W.; Chun, Y.; Shim, H.; Kwon, H.; Kim, J.; Kee, I.; Kim, S.; Lee, S.; et al. A Highly Sensitive Capacitive Touch Sensor Integrated on a Thin-Film-Encapsulated Active-Matrix OLED for Ultrathin Displays. *IEEE Trans. Electron Devices* **2011**, *58*, 3609−3615.

(6) Sai Bharadwaj, V. Y.; Sastry, V. N. Analysis on Sensors in a Smart Phone-Survey. *Int. J. Innovative Res. Adv. Eng.* **2014**, *1*, 96−108.

(7) Baxter, L. K. *Capacitive Sensors: Design and Applications*, 1st ed.; Herrickm, R. J., Ed.; Wiley−IEEE Press: New York, 1996; p 320.

(8) Hu, L.; Kim, H. S.; Lee, J.-Y.; Peumans, P.; Cui, Y. Scalable Coating and Properties of Transparent, Flexible, Silver Nanowire Electrodes. *ACS Nano* **2010**, *4*, 2955−2963.

(9) Singh, M.; Haverinen, H. M.; Dhagat, P.; Jabbour, G. E. Inkjet Printing-Process and Its Applications. *Adv. Mater.* **2010**, *22*, 673−685.

(10) Teichler, A.; Perelaer, J.; Schubert, U. S. Inkjet Printing of Organic Electronics − Comparison of Deposition Techniques and State-of-the-Art Developments. *J. Mater. Chem. C* **2013**, *1*, 1910.

(11) Triambulo, R. E.; Cheong, H.-G.; Lee, G.-H.; Yi, I.-S.; Park, J.-W. A Transparent Conductive Oxide Electrode with Highly Enhanced Flexibility Achieved by Controlled Crystallinity by Incorporating Ag Nanoparticles on Substrates. *J. Alloys Compd.* **2015**, *620*, 340−349.

(12) Lipomi, D. J.; Lee, J. A.; Vosgueritchian, M.; Tee, B. C.-K.; Bolander, J. A.; Bao, Z. Electronic Properties of Transparent Conductive Films of PEDOT:PSS on Stretchable Substrates. *Chem. Mater.* **2012**, *24*, 373−382.

(13) Takamatsu, S.; Takahata, T.; Muraki, M.; Iwase, E.; Matsumoto, K.; Shimoyama, I. Transparent Conductive-Polymer Strain Sensors for Touch Input Sheets of Flexible Displays. *J. Micromech. Microeng.* **2010**, *20*, 075017.

(14) Noh, J.; Yeom, D.; Lim, C.; Cha, H.; Han, J.; Kim, J.; Park, Y.; Subramanian, V.; Cho, G. Scalability of Roll-to-Roll Gravure-Printed Electrodes on Plastic Foils. *IEEE Trans. Electron. Packag. Manuf.* **2010**, *33*, 275−283.

(15) Krebs, F. C.; Fyenbo, J.; Jørgensen, M. Product Integration of Compact Roll-to-Roll Processed Polymer Solar Cell Modules: Methods and Manufacture Using Flexographic Printing, Slot-Die Coating and Rotary Screen Printing. *J. Mater. Chem.* **2010**, *20*, 8994.

(16) Facchetti, A. Printed Diodes Operating at Mobile Phone Frequencies. *Proc. Natl. Acad. Sci. U. S. A.* **2014**, *111*, 11917−11918.

(17) Ma, S.; Liu, L.; Bromberg, V.; Singler, T. J. Electroless Copper Plating of Inkjet-Printed Polydopamine Nanoparticles: A Facile Method to Fabricate Highly Conductive Patterns at near Room Temperature. *ACS Appl. Mater. Interfaces* **2014**, *6*, 19494−19498.

(18) Hermerschmidt, F.; Papagiorgis, P.; Savva, A.; Christodoulou, C.; Itskos, G.; Choulis, S. A. Inkjet Printing Processing Conditions for Bulk-Heterojunction Solar Cells Using Two High-Performing Conjugated Polymer Donors. *Sol. Energy Mater. Sol. Cells* **2014**, *130*, 474−480.

(19) Eperon, G. E.; Burlakov, V. M.; Docampo, P.; Goriely, A.; Snaith, H. J. Morphological Control for High Performance, Solution-Processed Planar Heterojunction Perovskite Solar Cells. *Adv. Funct. Mater.* **2014**, *24*, 151−157.

(20) Hilder, M.; Winther-Jensen, B.; Clark, N. B. Paper-Based, Printed Zinc−air Battery. *J. Power Sources* **2009**, *194*, 1135−1141.

(21) Janoschka, T.; Teichler, A.; Häupler, B.; Jähnert, T.; Hager, M. D.; Schubert, U. S. Reactive Inkjet Printing of Cathodes for Organic Radical Batteries. *Adv. Energy Mater.* **2013**, *3*, 1025−1028.

(22) Komoda, N.; Nogi, M.; Suganuma, K.; Otsuka, K. Highly Sensitive Antenna Using Inkjet Overprinting with Particle-Free Conductive Inks. *ACS Appl. Mater. Interfaces* **2012**, *4*, 5732−5736.



DOI: 10.1021/acsami.5b04717
*ACS Appl. Mater. Interfaces* 2015, 7, 21628−21633

(23) Yu, S. H.; Kim, B. J.; Kang, M. S.; Kim, S. H.; Han, J. H.; Lee, J. Y.; Cho, J. H. In/Ga-Free, Inkjet-Printed Charge Transfer Doping for Solution-Processed ZnO. *ACS Appl. Mater. Interfaces* **2013**, *5*, 9765−9769.
(24) Fukuda, K.; Sekine, T.; Kumaki, D.; Tokito, S. Profile Control of Inkjet Printed Silver Electrodes and Their Application to Organic Transistors. *ACS Appl. Mater. Interfaces* **2013**, *5*, 3916−3920.
(25) Kawase, T.; Shimoda, T.; Newsome, C.; Sirringhaus, H.; Friend, R. H. Inkjet Printing of Polymer Thin Film Transistors. *Thin Solid Films* **2003**, *438*−*439*, 279−287.
(26) Kawahara, Y.; Hodges, S.; Cook, B. S.; Zhang, C.; Abowd, G. D. Instant Inkjet Circuits. In *Proceedings of the 2013 ACM International Joint Conference on Pervasive and Ubiquitous Computing−UbiComp '13*; ACM Press: New York, 2013; p 363.
(27) Olberding, S.; Gong, N.-W.; Tiab, J.; Paradiso, J. A.; Steimle, J. A Cuttable Multi-Touch Sensor. In *Proceedings of the 26th Annual ACM Symposium on User Interface Software and Technology−UIST '13*; ACM Press: New York, 2013; pp 245−254.
(28) Barrett, G.; Omote, R. Projected-Capacitive Touch Technology. *Inf. Disp.* **2010**, *26*, 16−21.



DOI: 10.1021/acsami.5b04717
*ACS Appl. Mater. Interfaces* 2015, 7, 21628−21633